BMC Plant Biology

RESEARCH

Open Access

TcMYB73, a salicylic acid-responsive R2R3-MYB transcription factor, positively regulates paclitaxel biosynthesis in *Taxus chinensis* in direct and indirect ways

Yifei Ren[1†], Donglin Liu[1†], Weicheng Zhao[1], Xinran Wang[1], Xiaoying Cao[1*] and Wen Wan[1*]

Abstract

Background Paclitaxel (Taxol) is an invaluable secondary metabolite extracted from *Taxus* species, wildly utilized in cancer therapeutics. Salicylic acid (SA), an important phytohormone, substantially elevates paclitaxel accumulation in *Taxus* cell suspension cultures. However, the molecular mechanisms governing SA-induced modulation of paclitaxel biosynthesis remain poorly elucidated. Our previous studies identified TcMYB73, an SA-responsive R2R3-MYB transcription factor (TF), which demonstrates a robust positive correlation with paclitaxel biosynthesis, implying its orchestrating role in this metabolic pathway.

Results Expression pattern analysis revealed that TcMYB73 displays predominant expression in lateral roots. Both overexpression and RNA interference (RNAi) of *TcMYB73* demonstrated its regulatory function in modulating key paclitaxel biosynthetic genes, including *taxadiene synthase* (*TASY*), *10-deacetylbaccatin III-10-O-acetyltransferase* (*DBAT*), and *3'-N-debenzoyl-2'-deoxytaxol-N-benzoyltransferase* (*DBTNBT*). Transient TcMYB73 overexpression in *Taxus* chinensis (*T.* chinensis) needles induced 2.38-, 2.87-, and 1.79-fold increases in 10-DAB, baccatin III, and paclitaxel accumulation, respectively, compared to controls. Additionally, yeast one-hybrid (Y1H), Electrophoretic Mobility Shift Assay (EMSA), chromatin immunoprecipitation-quantitative PCR (ChIP-qPCR), and dual-luciferase (Dual-LUC) assays verified that TcMYB73 directly binds to MYB recognition elements in the *T10OH* promoter, enhancing its transcription. Furthermore, *TcWRKY33*, a transcriptional activator of *DBAT*, functions as a positive regulator mediating SA signaling within the paclitaxel biosynthetic pathway. Subsequent investigations validated that TcMYB73 upregulates *DBAT* expression via direct transcriptional activation of *TcWRKY33*. Collectively, these results demonstrate that *TcMYB73* transduces SA signals to *T10OH* and *TcWRKY33*, coordinately regulating paclitaxel biosynthesis through dual mechanisms: direct activation of biosynthetic genes and indirect modulation of upstream regulators.

Conclusions Our results indicated that the SA-responsive R2R3-MYB TF, TcMYB73 transcriptionally governs paclitaxel biosynthesis in *T. chinensis* through direct activation the expression of the *T10OH* gene, and activating *TcWRKY33* expression, thereby modulating *DBAT* expression. This study provides mechanistic insights into the role of TcMYB73 in mediating SA-induced transcriptional regulation of paclitaxel biosynthesis in *Taxus* species.

Keywords Taxus chinensis, R2R3-MYB transcription factor, Paclitaxel biosynthesis, Salicylic acid signal, TcWRKY33

†Yifei Ren and Donglin Liu contributed equally to this work.

*Correspondence:
Xiaoying Cao
cxy4868@jsnu.edu.cn
Wen Wan
wanwen85@jsnu.edu.cn

Background

Paclitaxel, marketed as Taxol®, is a renowned broad-spectrum chemotherapeutic agent employed as a first-line treatment for various solid malignancies, including breast, ovarian and lung cancers [1, 2]. This specialized diterpenoid compound is primarily isolated from yews (*Taxus* spp.), a genus of coniferous plants with significant medicinal value. However, akin to the productions of other plant-derived secondary metabolites such as vinblastine and artemisinin, paclitaxel occurs in minute quantities within *Taxus* tissues, yielding merely 40 mg per kilogram of bark [3]. Moreover, the chemical synthesis of paclitaxel, a molecular structure ranked among the most intricate plant-derived compounds, remains economically unfeasible [4]. Contemporary industrial production predominantly employs a semi-synthetic methodology, leveraging precursors like baccatin III and 10-deacetyl-baccatin III (10-DAB) sourced from *Taxus* cell cultures or unprocessed biomass, followed by catalytic conversion into the active pharmaceutical ingredient [5]. Projections estimate over 28 million new cancer diagnoses globally within the next two decades [6]. Despite its utility, the semi-synthesis strategy, constrained by reliance on slow-growing *Taxus* specimens and labor-intensive cell cultures, fails to satisfy the escalating demand for this potent oncotherapeutic [7]. Alternative approaches, such as *Taxus* cell culture biomanufacturing, offer fundamental prospects for scalable production. Nevertheless, transformative progress in resolving paclitaxel supply limitations hinges critically on elucidating the transcriptional regulation orchestrating its intricate biosynthetic pathway.

The paclitaxel biosynthetic pathway comprises approximately 20 enzymatic reactions initiated from geranylgeranyl pyrophosphate (GGPP), stratified into early, intermediate, and late stages. During the early phase, taxadiene synthase catalyzes the diterpenoid precursor GGPP into taxadiene (taxa-4(5),11(12)-diene,15), a foundational C20 terpenoid scaffold [8]. Subsequently, taxadiene undergoes sequential modifications in the intermediate stage via a conserved series of enzymes: 2α-, 5α-, 7β-, 9α-, 10β-, and 13α-hydroxylases, taxadienol 5α-O-acetyl transferase (TAT) and 10-deacetylbaccatin III 10-O-acetyltransferase (DBAT), culminating in the synthesis of the core intermediate baccatin III [9]. The terminal biosynthetic phase involves two critical processes: (1) generation of the side-chain precursor by phenylalanine aminomutase (PAM), activated via β-phenylalanine-CoA ligase-mediated conjugation to coenzyme A (CoA), and (2) stereospecific coupling of the side chain to baccatin III by baccatin III:3-animo-3-phenylpropanoyl transferase (BAPT), yielding 3′-N-dehydroxydebenzoylpaclitaxel. Final maturation of paclitaxel requires C2′-position hydroxylation by a cytochrome P450 hydroxylase, followed by regiospecific benzoylation via 3'-N-debenzoyl-2'-deoxytaxol-N-benzoyltransferase (DBTNBT) [9]. Recent advancements, including high-quality chromosome-level *Taxus* reference genomes [10–12], and transcriptomic profiling of paclitaxel pathway genes, have elucidated critical nodes in this orchestrated biosynthetic cascade [7, 13, 14]. Consequently, deciphering the transcriptional regulation governing paclitaxel biosynthesis represents a pivotal frontier with transformative potential for addressing global supply constraints.

The phytohormones salicylic acid (SA) and jasmonic acid (JA) are essential plant hormones that mediate immunity against pathogens [15]. Paclitaxel, a valuable secondary metabolite, serves as a crucial defense compound in *Taxus* plants, protecting against pathogen invasion and herbivory [16]. It is well-established that methyl jasmonate (MeJA) elicitation in *Taxus* cell cultures induces a broad upregulation of paclitaxel biosynthesis [17, 18]. Nearly all genes in the paclitaxel bioynthesis pathway, except for GGPPS and CoA Ligase, are markedly upregulated following JA elicitation [19]. To date, a series of transcription factors belonging to the WRKY, bHLH and ERF families have been implicated in the MeJA signaling cascade, where they orchestrate the expression of paclitaxel biosynthesis genes. Within the WRKY family, Li et al. [20] demonstrated that TcWRKY1, belongs to group I of the WRKY family, binds to two W-box motifs in the *DBAT* promoter region, potentiating its expression in *T. chinensis*. Similarly, TcWRKY26 (also a group I WRKY TF), directly regulates *DBAT* and forms a TcJAV3-TcWRKY26 complex, medicating an alternative JA signaling pathway involved in paclitaxel biosynthesis [21]. In the bHLH family, JAMYC1, JAMYC2, and JAMYC4 in *T. cuspidata* exhibit the capacity to suppress genes, such as *BAPT*, via binding to G and E-boxes [22]. Conversely, TcMYC2a in *T. chinensis* robustly regulates *TASY* by interacting with G-like boxes in its promoter. Among ERF TFs, two factors: TcERF12 (a repressor) and TcERF15 (an activator) modulate paclitaxel biosynthesis by targeting GCC-box elements on the *TASY* promoter [23]. Additionally, SA, is a recognized elicitor of paclitaxel biosynthesis [24, 25]. In response to SA, genes associated with paclitaxel biosynthesis are upregulated, resulting in significant accumulation of paclitaxel in *Taxus* cells [24–26]. For instance, Yu et al. [25]. demonstrated that supplementing *T. chinensis* cell cultures with SA (60 mg/L) and a fungal elicitor (50 mg/L) elevated paclitaxel levels to 11.5 mg/L, a 7.5-fold increase compared to the control. Similarly, Marziyeh et al. [26] observed that pre-treatment of *T. baccata* cell cultures with SA (5 mM) in a 2% glucose medium enhanced paclitaxel production by 5.1-fold and total taxanes by 3.5-fold.

To date, only one transcription factor, TcWRKY33, has been identified as involved in the SA signaling pathway, where it potentially regulates paclitaxel biosynthetic gene expression. In *T. chinensis*, TcWRKY33 promotes paclitaxel accumulation by directly activating the expressions of *DBAT* and the *TASY* activator *TcERF15* [27]. Furthermore, miR5298b has been implicated in SA-mediated regulation of paclitaxel biosynthesis. TcNPR3, a homolog of the SA receptor AtNPR3/4 is strongly induced by SA; miR5298b cleaves TcNPR3 mRNA, attenuating the inhibitory effect of the TcNPR3–TcTGA6 complex and thereby enhancing paclitaxel biosynthesis [28, 29]. Nevertheless, the SA-mediated regulatory mechanisms governing paclitaxel production in *Taxus* spp. remain incompletely elucidated.

MYB transcription factors, representing one of the largest TF families in plants, possess a highly conserved DNA-binding domain termed the MYB domain [30]. MYB proteins are categorized into four structural classes based on the number and arrangement of tandem repeats: 1R-MYB (R1/R2- and R3-MYB), 2R-MYB (R2R3-MYB), 3R-MYB (R1R2R3-MYB) and 4R-MYB (R1R2R2R1/2-MYB) [30]. R2R3-MYBs, which constitute the majority of MYB members, are implicated in diverse physiological processes, including primary and secondary metabolism, hormone signaling, and responses to biotic/abiotic stress. Notably, R2R3-MYB TFs exert pivotal regulatory roles in the biosynthesis and accumulation of specialized metabolites in medicinal plants [31]. Several R2R3-MYBs are involve in SA-mediated regulation of secondary metabolite biosynthesis. For instance, *CaMYB31*, a R2R3-MYB TF in *Capsicum annuum*, responds to SA signaling and acts as a positive regulator of capsaicinoid biosynthesis [32]. In *Taxus* species, R2R3-MYB TFs also linked to paclitaxel biosynthesis [33–36]. Three members: TmMYB3, TcMYB29a and TmMYB39, function as transcriptional activators of this pathway [33–35]. TmMYB3, a phloem-specific R2R3-MYB TF isolated from *T. media*, enhances paclitaxel production by upregulating *TmTBT* and *TmTS* expression [33]. TcMYB29a from *T. chininesis* binds the *T5OH* promoter, promoting paclitaxel biosynthesis via ABA signaling [34]. Yu et al. [35] identified TmMYB39, a female-specific R2R3-MYB in *T. media*, which directly activates paclitaxel biosynthesis genes (*TmGGPPS*, *TmT13αH*, *TmT10βH*, and *TmTBT*). Yeast two-hybrid (Y2H) and bimolecular fluorescence complementation (BiFC) assays revealed that TmMYB39 interacts with TmbHLH13 to form a heterodimeric complex, improving *TmGGPPS* and *TmT10βH* promoter activity, thus highlighting its role in transcriptional regulation via MYB-bHLH module. Additionally, endodermal cell-specific MYB47 is a putative activator of paclitaxel biosynthesis [37]. However, the SA-mediated transcriptional networks governing paclitaxel biosynthesis remain poorly characterized. Elucidating these mechanisms in *Taxus* species is critical for optimizing the utilization of taxane-producing plant resources.

In our previous research, we analyzed the transcriptomic responses of *T. chinensis* cell cultures to fungal elicitors and identified a nuclear-localized R2R3-MYB transcription factor, TcMYB73, which exhibited a strong correlation with paclitaxel biosynthesis, suggesting its regulatory potential in this pathway. In the present study, we investigated the functional role of TcMYB73 in modulating paclitaxel biosynthesis. *TcMYB73* is inducted by SA elicitation and its impact on taxane accumulation was validated through overexpression and RNAi experiments. The expression patterns of *TcMYB73* and transcript levels of paclitaxel pathway genes were quantified via quantitative real-time PCR (qPCR). To elucidate the molecular mechanisms, we employed YIH, EMSA, ChIP-qPCR and dual-luciferase reporter systems. These approaches revealed that TcMYB73 directly binds to the promoters of paclitaxel-biosynthesis related genes, activating their transcription. This study broadens our understanding of the regulatory roles of R2R3-MYB TFs, particularly TcMYB73, in medicating SA signaling to enhance paclitaxel biosynthesis in *Taxus* spp. Our findings underscore its significance as a transcriptional activator and provide novel insights into the SA-linked regulatory network governing taxane production.

Results

TcMYB73 is a nuclear-localized SA-Responsive R2R3-MYBtranscription factor highly expressed in lateral roots

TcMYB73 encodes a 233 amino acid protein with a predicted molecular weight of 26.79 kDa and a theoretical pI of 7.69. Sequence alignment revealed that the putative TcMYB73 contains two conserved R motifs in its N-terminal region, classifying it as an R2R3-MYB protein. To contextualize its evolutionary significance, a BLAST search against the SWISS-Prot database showed that TcMYB73 shares the highest sequence similarity (64.03%) with *T. c*hinensis R2R3 transcription factors 47 (QHG11475.1). Furthermore, phylogenetic analysis revealed a greater similarity among TcMYB73, TcMYB65, and TcMYB47 (Fig. 1a). To resolve broader evolutionary relationships, a neighbor-joining phylogenetic tree was generated using MEGA11.0, incorporating TcMYB73, 72 R2R3-TcMYBs, and 139 R2R3-AtMYB proteins from *T. chinensis* and *Arabidopsis thaliana* (Additional file 1). Notably, TcMYB73, TcMYB47 and TcMYB65 clustered within the *T. chinensis*-specific S33 subgroup, highlighting their potential functional divergence from other MYB proteins [38].

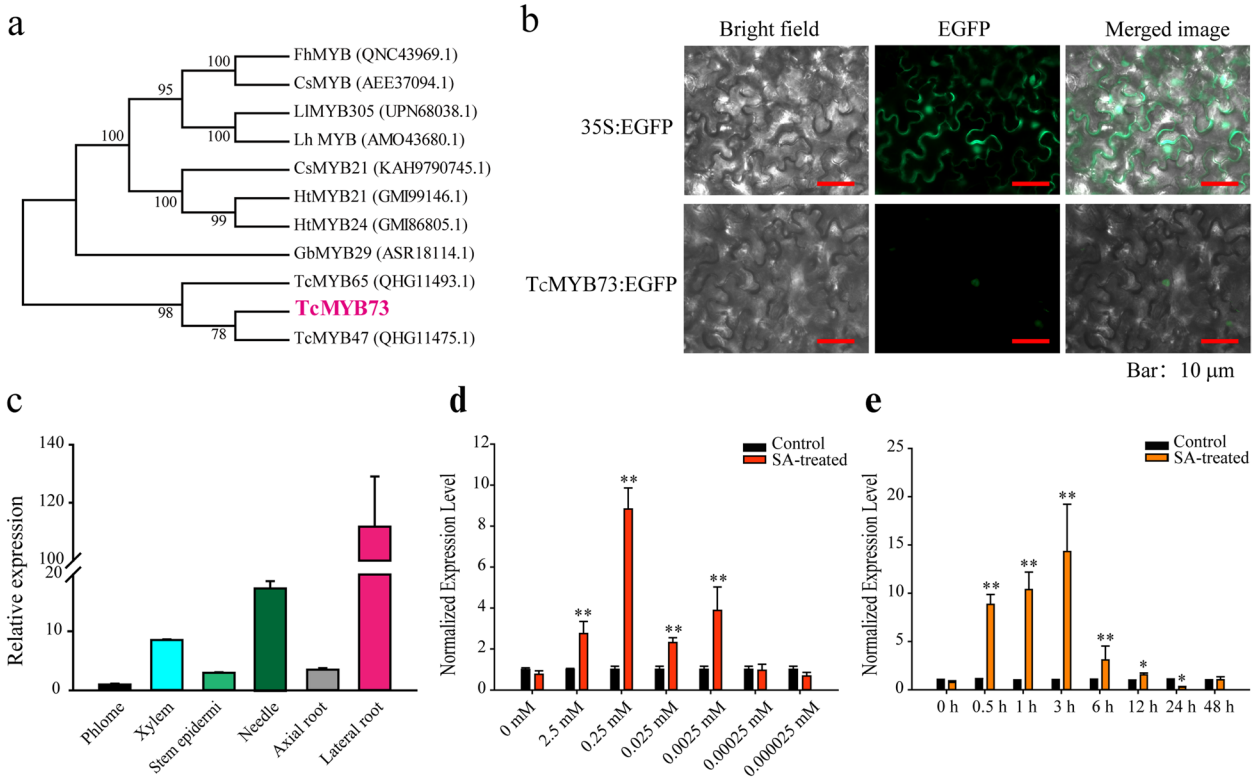

Fig. 1 Phylogenetic analysis, subcelular localization, and expression patterns of *TcMYB73*. **a** Phylogenetic tree of TcMYB73. Evolutionary relationships were inferred from full-length TcMYB73; TcMYB73 is highlighted in red. Reference sequences include: *Freesia hybrid* cultivar R2R3-MYB transcription factor (QNC43969.1), *Crocus sativus* MYB transcription factor (AEE37094.1), *Lilium longiflorum* transcription factor MYB305 (UPN68038.1), *Lilium hybrid* cultivar R2R3-MYB transcription factor (AMO43680.1), *Hibiscus trionum* myb domain protein 24 (GMI86805.1), *Citrus sinensis* transcription factor MYB21 (KAH9790745.1), *Hibiscus trionum* myb domain protein 21 (GMI99146.1), *Hibiscus trionum* myb domain protein 24 (GMI86805.1), *Ginkgo biloba* R2R3-MYB29 (ASR18114.1), *T. chinensis* R2R3-MYB transcription factor 47 (QHG11475.1), and *T. chinensis* R2R3-MYB transcription factor 65 (QHG11493.1). **b** Subcellular Localization of the TcMYB73 protein. For subcellular localization, the EGFP-TcMYB73 fusion construct was transiently expressed in tobacco epidermal cells. EGFP fluorescence was visualized 48–72 h post-transfection using a Leica fluorescence microscope (OLYMPUS, Japan). **c** Tissue-specific expression of the *TcMYB73* gene in six *T. chinensis* tissues via qPCR. *TcGAPDH* served as the internal control. **d** Expression analysis of *TcMYB73* under varying SA concentrations. **e** Temporal expression profile of *TcMYB73* following 0.25 mM SA treatment. Suspended *T. chinensis* cells were exposed to 0.25 mM SA, with ethanol solvent as the negative control. Transcript levels of *TcMYB73* were quantified at 0, 0.5, 1, 3, 6, 12, 24, and 48 h post-treatment. Normalized expression levels (relative to solvent-treated controls) are displayed on the ordinate, with *TcGAPDH* serving as the reference gene. Error bars represent mean ± standard deviation (SD) derived from three replicates ($n = 3$)

Subcellular localization assays in tobacco leaf epidermal cells transiently expressing EGFP-TcMYB73 confirmed nuclear enrichment of GFP fluorescence (Fig. 1b). In contrast, control cells expressing free EGFP exhibited fluorescence in both cytoplasm and nucleus (Fig. 1b). This nuclear specificity aligns with the canonical role of R2R3-MYB proteins as DNA-binding transcription factors. Tissue-specific qPCR analysis further demonstrated that *TcMYB73* transcript abundance in lateral roots markedly exceeded levels in other tissues (Fig. 1c). Collectively, these results findings establish TcMYB73 as a nuclear-localized R2R3-MYB TF with pronounced expression in lateral roots.

To evaluate the responsiveness of *TcMYB73* to SA in *T. chinensis* callus, we quantified *TcMYB73* transcript levels via qPCR. Figure 1d illustrates the relative expression of TcMYB73 in *Taxus* cells treated with varying SA concentrations. Notably, TcMYB73 expression increased significantly, reaching an 8.83-fold induction relative to untreated controls following exposure to 0.25 mM SA. Subsequent analysis of the time-dependent response to 0.25 mM SA revealed that TcMYB73 expression peaked at 3 h (14.32-fold induction) before gradually declining (Fig. 1e). These findings confirm that TcMYB73 responds rapidly and robustly to SA signaling.

TcMYB73 upregulates ten genes involved in paclitaxel biosynthesis thereby augmenting the production of paclitaxel

As a transcription factor, TcMYB73's overexpression likely modulates downstream target gene, expression, thereby promoting taxane accumulation. Paclitaxel

biosynthesis entails a complex pathway comprising approximately 19 enzymatic steps, and over 20 enzymes (Fig. 2a). To elucidate the regulatory role of TcMYB73 in this pathway, we transiently overexpressed *TcMYB73* in *Taxus* needles and quantified transcript levels of paclitaxel biosynthesis genes via qPCR. In transformed needles, *TcMYB73* expression demonstrated a 62.11-fold increase relative to untreated control (Fig. 2b). Similarly, transcriptional upregulation was observed for key biosynthetic genes (*DXS*, *TASY*, *T5OH*, *T10OH*, *T13OH*, *TAT*, *DBAT*, *BAPT*, *PAM* and *DBTNBT*) with expression levels elevated by 1.95-, 1.99-, 2.85-, 3.22-, 3.92-, 2.79-, 1.88-, 2.37-, 2.64-, and 2.00-fold, respectively, compared to the controls (Fig. 2b). To further validate these findings, *TcMYB73* expression was suppressed in fresh *Taxus* needles using transient RNAi. RNAi-treated needles exhibited a 0.38-fold reduction in *TcMYB73* transcript levels (Fig. 2c). Correspondingly, most paclitaxel biosynthesis genes, including *DXS*, *DXR*, *TASY*, *T5OH*, *T10OH*, *TAT*, *BAPT* and *DBTNBT*, showed marked downregulation, with expression levels reduced to 0.13-, 0.52-, 0.01-, 0.03-, 0.56-, 0.08-, 0.43-, 0.03- and 0.34-fold of control values (Fig. 2c). These results demonstrate that *TcMYB73* significantly enhances the transcription of paclitaxel biosynthesis genes, particularly critical enzymes such as *TS*, *DBAT* and *DBTNBT*.

To assess the regulatory role of *TcMYB73* in paclitaxel biosynthesis, we measured taxanes levels including 10-DAB, baccatin III and paclitaxel, in *T. chinensis* needles transiently overexpressing (*TcMYB73-OE)* or silencing (*TcMYB73-RNAi*) TcMYB73. Overexpression increased taxane concentrations to 691.23 ± 68.68 μg/g dry weight (DW) (10-DAB), 43.85 ± 4.18 μg/g DW (Baccatin III) and 155.10 ± 17.88 μg/g DW (paclitaxel), corresponding to 2.38-, 2.87- and 1.79-fold increases relative to controls, respectively (Fig. 2d). Conversely, *TcMYB73* knockdown reduced 10-DAB, baccatin III and paclitaxel levels to 0.85-, 0.81- and 0.70-fold of controls, respectively (Fig. 2e), though these reductions lacked statistical significance. Collectively, these data demonstrate that the SA-responsive transcription factor TcMYB73 positively regulates paclitaxel biosynthesis.

TcMYB73 directly activates *T10OH* by binding to MRE in its promoter

To identify candidate target genes, promoter sequences of all ten genes were scanned for potential MYB-recognition elements (MREs). DNA fragments (250–400 bp) containing putative MREs from these promoters were cloned into the pLacZ(2μ) plasmid for Y1H assays. Screening on SD/-Trp/-Ura/Gal/Raf/X-Gal medium revealed that TcMYB73 physically bound to a promoter fragment of *T10OH* (Fig. 3a). Furthermore, colony color intensity diminished in the Y1H assay upon mutation of the MRE1 site, suggesting that TcMYB73 physically interacts with MRE1 in the *T10OH* promoter (Fig. 3a).

Then, EMSAs were performed to validate this interaction. A biotinylated probe containing MRE1 from the *T10OH* promoter was incubated with recombinant TcMYB73 N-GST. Binding resulted in distinct mobility shifts, which were competitively inhibited by unlabeled probes but not by mutated sequences (Fig. 3b). No shifts occurred when the probe was incubated with GST alone (Fig. 3b), confirming that TcMYB73 specifically binds to the *T10OH* promoter. ChIP-qPCR further corroborated in vivo binding, showing significant enrichment of the MRE1-containing promoter region with a TcMYB73-GFP antibody compared to the control IgG (Fig. 3c). Collectively, Y1H, EMSA, and ChIP-qPCR data demonstrate that *T10OH* is a downstream target of TcMYB73.

To assess the transcriptional activity of TcMYB73 in vivo, Dual-LUC assays were employed. Co-expressed of pBD-TcMYB73 with a *LUC* reporter construct significantly enhanced luciferase activity compared to the negative control (pBD), reaching levels akin to the positive control (pBD-VP16; Fig. 3d). This confirms TcMYB73's role as a transcriptional activator.

Dual-LUC assays were employed to access the transcriptional regulation of the candidate target gene *T10OH* by TcMYB73 in plant cells. As shown in Fig. 3e, TcMYB73 strongly activated the pT10OH-LUC reporter compared to the empty vector, indicating that TcMYB73 functions as a transcriptional activator by directly binding to the promoter regions of *T10OH* gene. Mutation of the MRE1 site drastically reduced LUC/REN ratios, indicating that MRE1 is indispensable for TcMYB73-mediated transcriptional activation (Fig. 3e).

TcMYB73 directly activates *TcWRKY33* by binding to the MREs in its promoter

The *DBAT* gene, which encodes a rate-limiting enzyme in paclitaxel biosynthesis, is transcriptionally upregulated by the TcMYB73 transcription factor. However, the *DBAT* promoter does not appear to be directly bound by T*cMYB73*, implying the involvement of an intermediary regulatory factor. Database analysis identified *TcWRKY33*, a SA-responsive positive regulator of *DBAT* containing two MREs in its promoter [27]. Transient overexpression of *TcMYB73* in *T. chinensis* needles induced a 2.09-fold upregulation of *TcWRKY33* transcript levels relative to controls (Fig. 2b). Conversely, *TcMYB73* RNAi in needles transiently reduced *TcWRKY33* expression to 0.18-fold of control levels, suggesting *TcWRKY33* is a downstream target of *TcMYB73* (Fig. 2c).

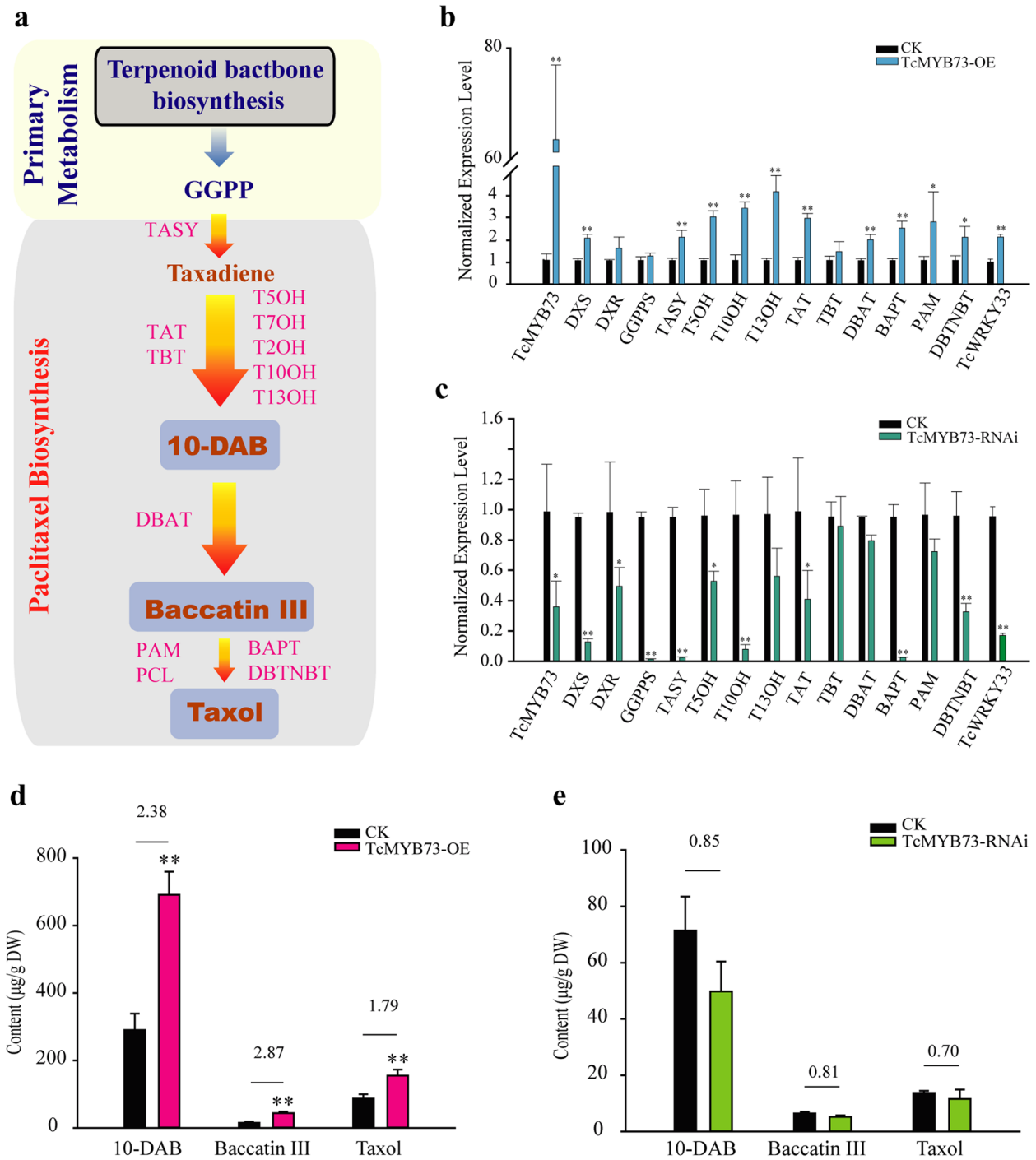

Fig. 2 TcMYB73 modulates the expression of paclitaxel biosynthesis-related genes in *T. chinensis* needles and enhances the paclitaxel biosynthesis. **a** The paclitaxel biosynthesis pathway. TASY: taxadiene synthase; TAT: taxadien 5α-ol-O-acetyl transferase; TBT: taxane 2α-O-benzoyl transferase; T5OH: taxane 5α-hydroxylase; T7OH: taxane 7β-hydroxylase; T2OH: taxane 2α-hydroxylase; T10OH: taxane 10β-hydroxylase; T13OH: taxane 13α-hydroxylase; DBAT: 10-deacetyl baccatin III 10β-O-acetyl transferase; PAM: phenylalanine aminomutase; PCL: phenylalanoyl CoA ligase; BAPT: baccatin III:3-animo-3-phenylpropanoyl transferase; and DBTNBT: 3′-N-debenzoyl-2′-deoxytaxol N-benzoyl transferase. Transcript levels of paclitaxel biosynthetic genes in *T. chinensis* needles subjected to *TcMYB73* overexpression (**b**) or RNAi silencing (**c**) were quantitatively assessed using qPCR. *TcGAPDH* was employed as the reference gene. Quantification of taxane metabolites (10-DAB, baccatin III and paclitaxel) in *T. chinensis* needles transiently overexpressing *TcMYB73* (**d**) and subjected to RNAi (**e**) as determined by liquid chromatography-mass spectrometry (LC–MS). Experiments included three biological replicates. Statistical significance was assessed using Student's *t*-test (*0.01 < p < 0.05, and **p < 0.01)

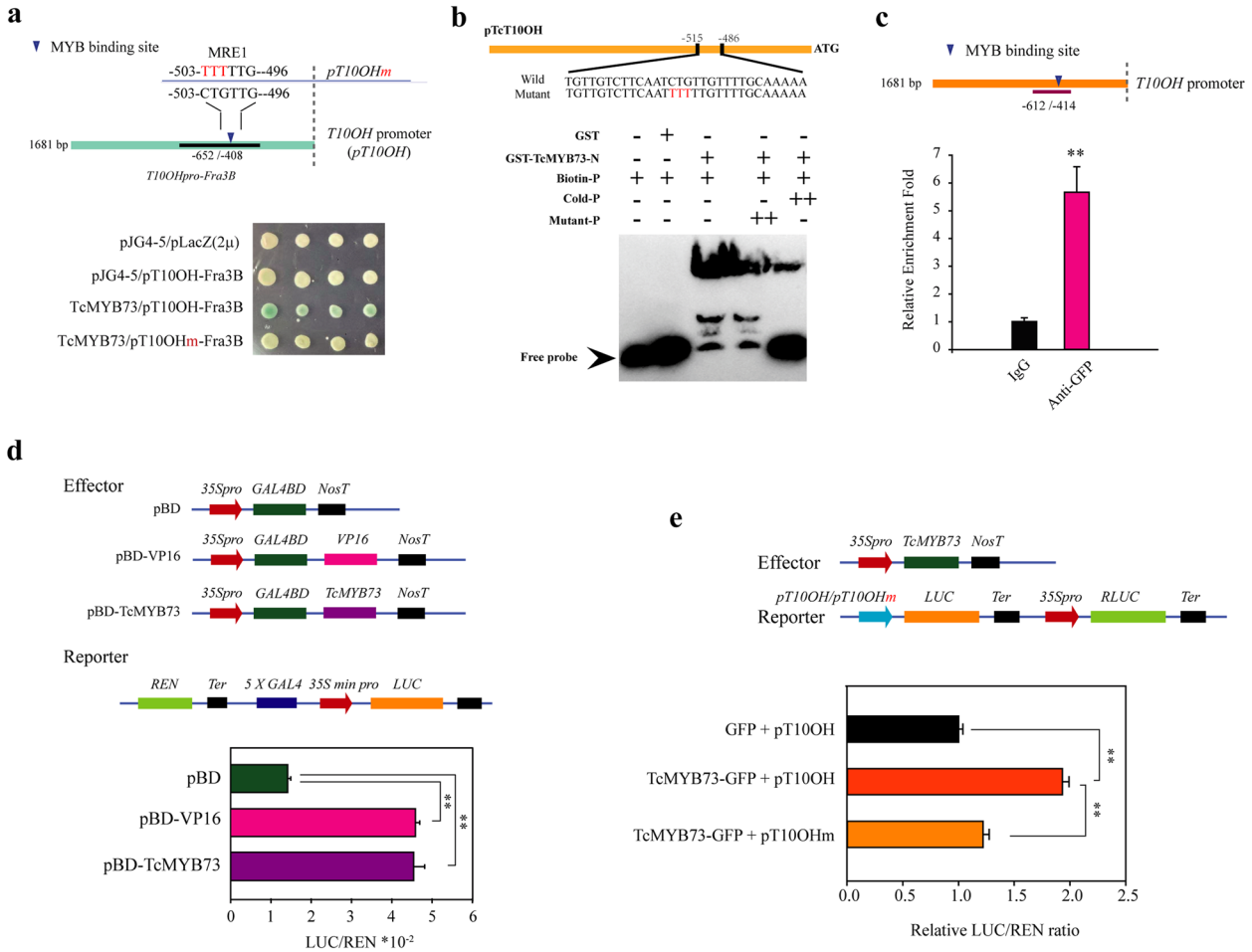

Fig. 3 TcMYB73 directly activated *T10OH* by binding to the MRE in its promoter. **a** Y1H analysis of TcMYB73 and MREs. Bait vector containing individual MREs were co-transformed with the empty pJG4-5 into yeast strain EGY48 as a negative control. The schematic illustrates the *T10OH* promoter, with a blue pentagons denoting the MRE1 motif. **b** EMSA. Competitor unlabeled probes (200:1 molar excess relative to biotin-labeled probes) were added (denoted by + +). **c** ChIP-qPCR. **d** A Dual-LUC assay evaluating the transcriptional activity capacity of TcMYB73. The effector constructs included pBD (negative control), pBD-TcMYB73, and pBD-VP16 (positive control). **e** Transient dual-luciferase reporter assays in tobacco leaves. The *TcMYB73* expression cassette, driven by the CaMV 35S promoter, was co-introduced with reporter plasmids into tobacco leaves. The LUC/REN enzymatic activity ratio was quantified. All experiments were performed in three triplicate. Data represent mean ± SD from three biological replicates. Statistical significance was determined using Student's *t*-test (**$p < 0.01$)

A 1500 bp 5'-flanking sequence of the *TcWRKY33* promoter isolated, with in silico tools predicting multiple MRE motifs. The promoter fragments contained the predicting MRE motifs (250–400 bp) were cloned into pLacZ(2μ) and co-transformed with a TcMYB73-AD fusion vector for Y1H assay. Screening on SD/-Trp/-Ura/Gal/Raf/X-Gal medium plates confirmed directly binding of TcMYB73 to the *TcWRKY33* promoter (Fig. 4a). Mutation of the MRE2 site within this promoter fragment abolished binding activity in Y1H assays, indicating TcMYB73 specifically interacts with MRE2 (Fig. 4a). EMSA further validated this interaction. Recombinant TcMYB73 N-GST bound to a *TcWRKY33* promoter fragment containing MRE2, causing mobility shifts that were competitively inhibited by unlabeled wild-type probes but not mutated sequences (Fig. 4b). No shifts occurred with GST alone, confirming binding specificity (Fig. 4b). ChIP-qPCR using a TcMYB73-GFP antibody revealed significant enrichment of the MRE2-containing *TcWRKY33* promoter region compared to controls (Fig. 4c). Collectively, Y1H, EMSA and ChIP-qPCR data demonstrate that MRE2 in the *TcWRKY33* promoter is a direct in vitro target of TcMYB73.

To assess functional relevance, full-length *TcWRKY33* promoter (*pWRKY33*) and one MRE2 mutated variant (*pWRKY33 m*) were co-transformed with TcMYB73 into *Nicotiana benthamiana* leaves respectively (Fig. 4d). LUC/REN ratios were significantly lower

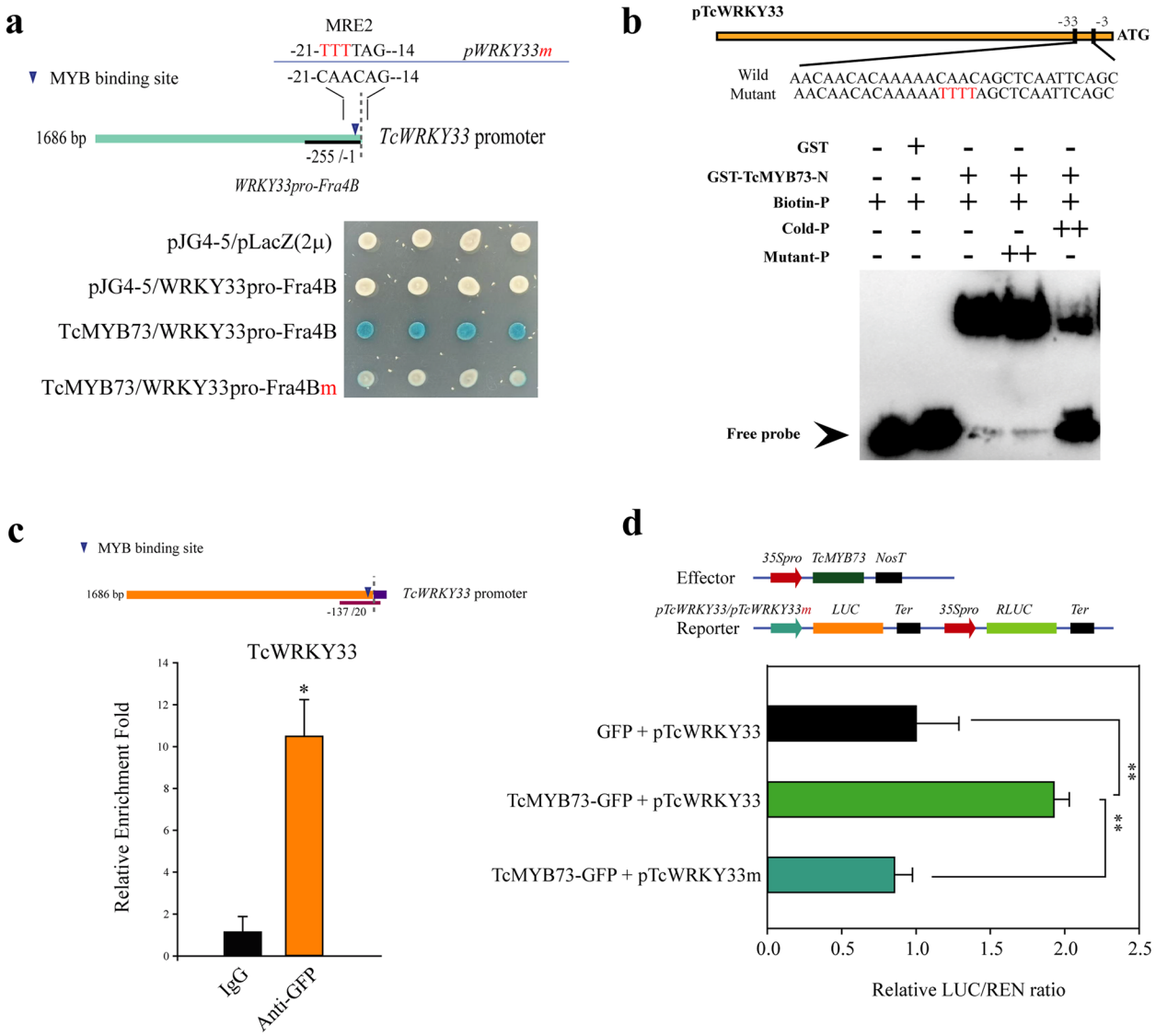

Fig. 4 TcMYB73 directly binds to the *TcWRKY33* promoter. **a** Y1H analysis of interactions between TcMYB73 and MRE motifs. Yeast strains was cultured on selective chromogenic media. **b** EMSA. Competitor unlabeled probes (200:1 molar excess relative to biotin-labeled probes) are denoted by + +. **c** ChIP-qPCR. Schematic representation of the *TcWRKY33* promoter, containing a single MRE (indicated by a blue pentacle). The full-length *TcWRKY33* promoter (*pWRKY33*) and a MRE2 mutated variant (*pWRKY33 m*) were engineered. **d** Transient Dual-LUC assays. The *TcMYB73* expression vector, driven by the CaMV 35S promoter, was co-transformed with reporter plasmids into tobacco leaves. LUC/REN activity ratios was quantified. All experiments was performed three replicates. Statistical significance was determined via Student's *t*-test (*0.01 < $p < 0.05$ and **$p < 0.01$)

for *pWRKY33 m* than *pWRKY33*, confirming that TcMYB73 activates transcription via MRE2 binding (Fig. 4d). These findings establish TcWRKY33, an SA-responsive paclitaxel biosynthesis regulator, as a direct transcriptional target of TcMYB73.

Discussions

Paclitaxel, a widely-used anticancer agent, is a high-value secondary metabolite predominantly extracted from *Taxus* species. However, its extremely low abundance in natural plant sources results in exorbitant production costs and a marked global supply–demand imbalance [3]. The phytohormone SA plays a regulatory role in paclitaxel biosynthesis within *Taxus* and stimulates

its accumulation [24, 25]. Nevertheless, the molecular mechanisms underlying SA-mediated modulation of this pathway remain poorly characterized. While R2R3-MYB transcription factors have been preliminarily explored for their roles in *Taxus* spp., several members of this family have been identified as key regulators of paclitaxel biosynthesis [33–37]. Despite this progress, the involvement of R2R3-MYB TFs in SA signal transduction pathways remains unelucidated. In this study, we identified and characterized *TcMYB73*, an SA-inducible R2R3-MYB TF, and investigated its function contribution to paclitaxel biosynthesis.

In this study, we demonstrated that TcMYB73 strongly enhances the accumulation of paclitaxel and its primary precursors, baccatin III and 10-DAB (Fig. 2d). Notably, transcription levels of most paclitaxel biosynthetic genes were markedly elevated upon *TcMYB73* overexpression (Fig. 2b), with pronounced upregulation of *TASY*, *DBAT*, and *DBTNBT*, which are encoding key enzymes in this pathway. Conversely, silencing *TcMYB73* significantly suppressed these genes, confirming its role as a key transcriptional regulator. These findings were further validated by functional assays (Fig. 3d), which established TcMYB73 as a transcriptional activator. This aligns with prior reports on R2R3-MYB transcription factors in *Taxus*, which similarly activate paclitaxel biosynthesis [33–35, 37].

Beyond genetic regulation, the spatial distribution of paclitaxel and its intermediates in *Taxus* tissues (e.g., bark, needles, roots) is influenced by species-specific traits, environmental conditions, plant age, sex, and harvest season [19, 39–43]. For instance, paclitaxel accumulates preferentially in root, trunk, and branch bark, whereas its precursors, 10-DAB and baccatin III, dominate in needles and stems [39, 43]. In *T. chinensis*, paclitaxel concentrations peak in bark and roots, while baccatin III is abundant in both mature and young needles [43]. This tissue-specificity correlates with differential expression of biosynthetic genes. In *T. chinensis*, *GGPPS* and *T10OH* (early pathway genes) are highly transcribed in fresh needles, whereas DBAT (a late-stage enzyme) is enriched in bark and roots [43]. Intriguingly, *Taxus yunnanensis* exhibits contrasting patterns, with *GGPPS* and *T10OH* predominantly expressed in roots and stems [19]. Our data further revealed elevated transcription of *TASY*, *DBAT*, and *DBTNBT* in lateral roots (Additional file 2), consistent with paclitaxel's preferential accumulation in roots. However, unlike Liu et al. [19], we observed minimal *T10OH* expression in *T. chinensis* needles, a discrepancy potentially attributable to differences in plant age, sampling season, or growth conditions. Systematic investigation of these variables is critical to unraveling paclitaxel accumulation mechanisms and optimizing industrial production, which need to be further studied.

Focusing on enzymatic regulation, T10OH catalyzes a pivotal hydroxylation step in the paclitaxel biosynthesis pathway, converting taxa-4 (20),11(12)-dien-5α-yl acetate into a key taxoid intermediate [44]. Using Y1H, EMSA, ChIP-qPCR, and Dual-LUC assays, we demonstrated that TcMYB73 binds to the MRE1 motif in the *T10OH* promoter, directly enhancing its transcription (Fig. 3). This activation increased 10-DAB levels, a precursor derived from upstream biosynthesis, by 2.38-fold. Similarly, *DBAT*, which mediates the rate-limiting conversion of 10-DAB to baccatin III [39], is indirectly regulated by TcMYB73. Notably, TcWRKY33, a known activator of *DBAT*, was upregulated in TcMYB73-OE needles. Promoter analysis and functional assays confirmed that TcMYB73 activates *TcWRKY33* by binding to an MRE site in its promoter, leading to a 2.87-fold increase in baccatin III (Figs. 2c and 4). These results, corroborated by qPCR and metabolite quantification (Figs. 2c and 4), establish that TcMYB73 elevates baccatin III levels through indirect upregulating *DBAT* expression. Collectively, our findings illustrate how TcMYB73 orchestrates paclitaxel biosynthesis by directly and indirectly modulating critical enzymatic steps.

The R2R3-MYB proteins of *T. chinensis* and *A. thaliana* are classified into 36 subgroups based on their evolutionary relationships and functional divergence. Among these, 24 subgroups include members from both species, while three are exclusive to *T. chinensis* and nine are unique to *A. thaliana* [38]. Notably, TcMYB73, TcMYB47, and TcMYB65 clustered within the S33 subgroup, which is specific to *T. chinensis* [38]. Previous studies have identified several R2R3-MYB TFs associated with paclitaxel biosynthesis, including *TcMYB29a* from *T. chinensis*, *TmMYB3* and *TmMYB39* from *T. media*, *TmMYB47*, *TmMYB65*, *TmMYB3R1*, *TmMYB56* and *TmMYB105* from *T. mairei* [33–37]. For instance, ABA-responsive TcMYB29a modulates paclitaxel accumulation in *T. chinensis* needles following fungal elicitation [34]. Similarly, TmMYB3, a phloem-specific R2R3-MYB TF, governs the phloem-specific biosynthesis of paclitaxel [33], whereas female-specific TmMYB39 enhances paclitaxel production by directly activating biosynthetic genes and forming the TmMYB39-TmbHLH13 regulatory complex via the MYB-bHLH module [35]. In *T. mairei*, TmMYB47, TmMYB65, TmMYB3R1, TmMYB56, and TmMYB105 collectively orchestrate the paclitaxel biosynthesis network [36, 37]. However, despite their shared regulatory roles, TcMYB29a, TcMYB3, TmMYB3 and TmMYB39 exhibit low amino acid sequence similarity (≤ 22.37% identity) (Additional file 3) and divergent expression patterns. For example, *TmMYB3* and

TmMYB39 are expressed phloem-specifically and female-predominantly expression, respectively, whereas *TcMYB29a* shows elevated expression in needles and roots, and *TcMYB73* is enriched in lateral roots (Fig. 1c). Furthermore, *TmMYB47* localizes to endodermal cells, while *TmMYB65*, *TmMYB56*, and *TmMYB105* are predominantly expressed in the mesophyll cells. These findings align with reports by Zhan et al. [36] and Cao et al. [34], who proposed that MYB TFs in *Taxus* exhibit cell-type specificity and may have independently evolved across tissues to regulate spatially distinct paclitaxel biosynthetic pathways. Importantly, our identification of *TcMYB73* extends the work of Hu et al. [38], who cataloged 72 MYB genes in *T. chinensis* but did not characterize this regulator. Thus, further genomic exploration of *T. chinensis* is warranted to elucidate the full regulatory network.

SA is a well-established inducer of paclitaxel biosynthesis in *Taxus* species and cell cultures [24–26]. To date, only one TF, *TcWRKY33*, has been linked to SA-mediated regulation of this pathway [27]. In this study, we demonstrate that *TcMYB73* responds robustly to SA signaling and transduces these signals to downstream paclitaxel biosynthetic genes, thereby promoting metabolite accumulation. Specifically, TcMYB73 regulates two critical genes (*T10OH* and *DBAT*) through distinct mechanisms. First, TcMYB73 directly binds to the MRE1 region of *T10OH* promoter in response to SA. Second, while *DBAT* is known to respond to SA signal [27], our data reveal that TcMYB73 significantly amplifies *DBAT* expression (Fig. 2b). Notably, TcMYB73 also activates *DBAT* indirectly by targeting *TcWRKY33*, a known activator of *DBAT*. Collectively, these results establish TcMYB73 as a dual regulator of SA signaling, coordinating both direct and indirect pathways to enhance paclitaxel biosynthesis (Fig. 5). Intriguingly, other pivotal genes, such as *TASY* and *DBTNBT*, exhibit upregulate expression in TcMYB73-OE needles (Fig. 2b), but are not directly regulated by TcMYB73.

Beyond SA, JA is another potent elicitor of paclitaxel biosynthesis, upregulating nearly all genes in the pathway [26]. Interestingly, promoter analysis of TcMYB73

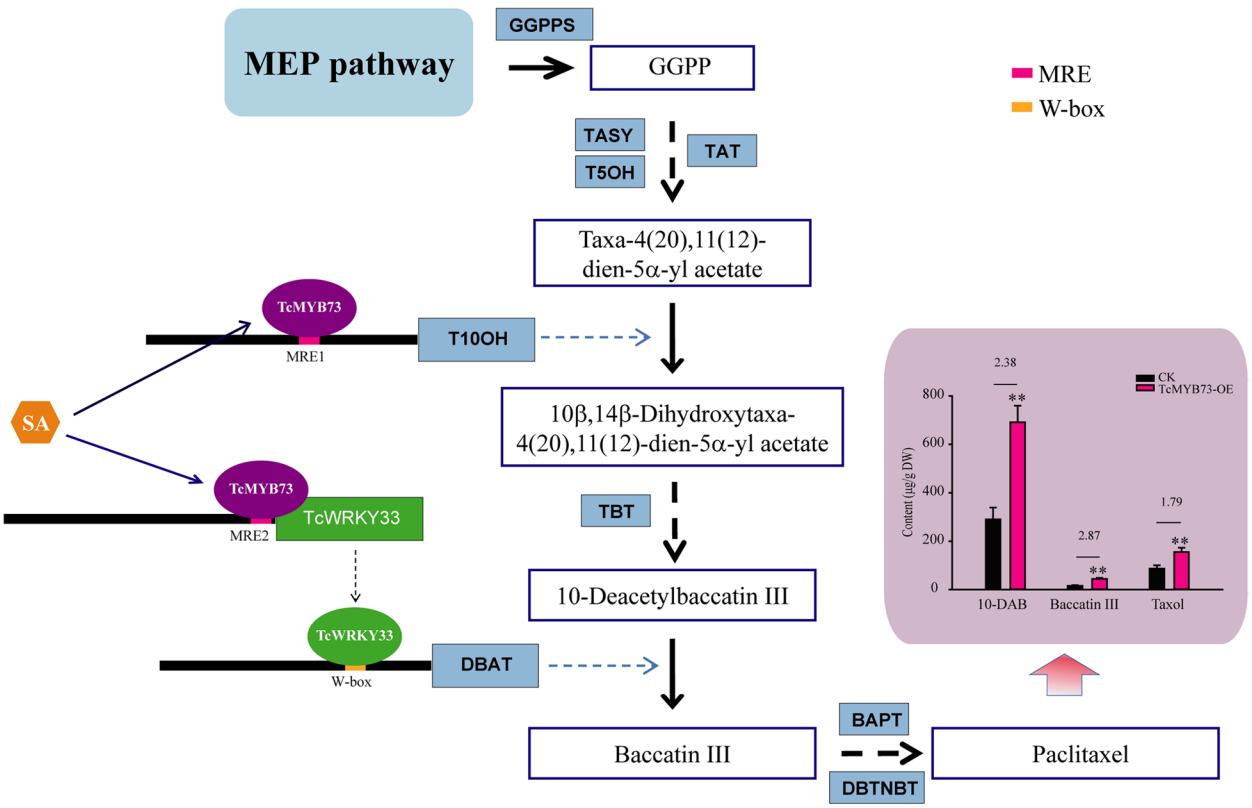

Fig. 5 Proposed mechanistic role of TcMYB73 in the transcriptional regulation of paclitaxel biosynthesis in *T. chinensis*. MEP: methylerythritol phosphate; GGPP: geranylgeranyl diphosphate; GGPPS: geranylgeranyl diphosphate synthase; TASY: taxadiene synthase; T5OH: taxane 5α-hydroxylase; T10OH: taxane-10β-hydroxylase; TAT: taxadienol 5α-O-acetyl transferase; TBT: taxane-2α-Obenzoyltransferase; DBAT: baccatin III:3-animo-3-phenylpropanoyl transferase; BAPT: baccatin III 13-O-(3-amino-3-phenylpropanoyl) transferase; DBTNBT: 3′-N-debenzoyl-2′-deoxytaxol-N-benzoyltransferase; SA, salicylic acid

identified a JA-responsive CGTCA motif (−507 to −511), and RNA-seq data (Accession No: CRA003496) [10] confirm that *TcMYB73* expression is markedly induced by JA. These observations imply that TcMYB73 may also mediate JA-regulated paclitaxel production, potentially influencing rate-limiting enzymes through yet uncharacterized pathways. Therefore, future studies should investigate how *TcMYB73* integrates multiple hormonal signals to fine-tune paclitaxel biosynthesis.

Pretreatment of *Taxus* cell cultures with SA enhances taxane biosynthesis while concurrently bolstering cellular health and stress resilience, thereby promoting higher yields during glucose and fungal elicitor treatments [25, 26]. These results highlight the pivotal role of SA in modulating secondary metabolite synthesis and metabolic homeostasis in *Taxus* cultures. Nevertheless, if the direct involvement of SA-responsive TFs, such as TcMYB73 and TcWRKY33, in these pathways remains unclear. Further investigation is required to elucidate the precise regulatory mechanisms and to determine how these TFs drive the observed increases in taxane accumulation and cellular viability.

Conclusions

TcMYB73 modulates paclitaxel biosynthesis in *T. chinensis* through dual mechanisms: directly transcriptional activation of the *T10OH* gene and indirect regulation of *DBAT* via interaction with *TcWRKY33* promoter. *TcMYB73* exhibits predominant expression in lateral roots relative to needles, phloem, xylem, and axial roots. These findings propose a plausible mechanism underlying the heightened accumulation of paclitaxel in *Taxus* lateral roots following fungal elicitor treatment. Upon SA application, transcript levels significantly increased, suggesting the existence of a previously unrecognized SA-dependent regulatory pathway for paclitaxel biosynthesis**,** distinct from the JA-mediated pathway.

Methods

Plant materials

T. chinensis seedlings (Jiangsu Yew Biotechnology Co., Ltd, Wuxi, China) were cultivated in soil-filled under controlled greenhouse at the Jiangsu Normal University (Xuzhou, China), at 22℃, a 12-h light/dark cycle, and 70% relative humidity. Tissue specimens (needles, stem epidermis, phloem, xylem, axial roots, and lateral roots were harvested from 2-year-old *T. chinensis* seedlings. All samples were flash-frozen in liquid nitrogen and preserved at −80℃ for subsequent analysis. Experiments were conducted with three or more biological replicates.

Taxus chinensis callus were induced from young stems of laboratory-cultivated seedlings following the protocol described by Lee et al. [45], and cultured in sterile containers containing modified Gamborg's B5 medium [45], supplemented with 20 g/L sucrose and 4 g/L phytagel. Callus cultures were incubated at 22℃ in darkness and subcultured every two weeks as previously described [34].

Phytohormone treatments

T. chinensis calli were employed for phytohormone exposure. Eight grams of callus cultures were transferred into B5 liquid medium and agitated at 100 rpm under a 48-h dark conditions. Cultures were supplemented with 2.5 mM SA or an equivalent volume of ethanol solvent (control). For transcriptional profiling, samples were collected at 0, 0.5, 1, 3, 6, 12, 24 and 48 h post-treatment, flash-frozen in liquid nitrogen, and stored at −80℃ until RNA extraction. The experiment included three biological replicates.

RNA extraction, cDNA synthesis, and cloning of the *TcMYB73* gene

Total RNA was isolated using the EASYspin plant RNA extraction kit (Aidlab Bio., China) following the manufacturer's protocol. First-strand cDNA was subsequently synthesized with HiScript II Q RT SuperMix with gDNase (Vazyme, China) according to the protocols of the manufacturer.

The *TcMYB73* gene sequence (Genebank ID: PV408260), containing a 702 bp open reading frame (ORF), was identified from our transcriptomic data (NCBI accession: PRJNA751266). Its deduced amino acid sequence exhibited a conserved R2R3-MYB domain. The full-length ORF was amplified via PCR from *T. chinensis* cDNA, employing primers designated TcMYB73-F/R (Additional file 4). Amplified products were purified, ligated into the pMD18-T vector (TaKaRa, Dalian, China) using T/A cloning, and sequenced for validation. Sequencing confirmed the successful insertion of the TcMYB73 ORF into the recombinant vector, which was designated pMD18-TcMYB73.

Sequence alignment and phylogenetic analysis of *TcMYB73*

The physicochemical properties of TcMYB73, including the amino acid count, molecular weight (MW), isoelectric point (pI), hydrophobicity, and instability index, were predicted using Prosite ExPASy server (http://web.expasy.org/protparam/). A homology search was conducted using the BLAST algorithm from the SWISS-PROT protein database (http://www.ncbi.nlm.nih.gov/BLAST/). The alignment and assessment of the percentage identity of TcMYB73 with known MYB proteins were executed using DNAMAN software (Version 9.0). Phylogenetic analysis was conducted using the neighbor-joining method with 1,000 bootstrap resamplings in MEGA

software version 11.0 (https://www.megasoftware.net/older_versions).

Subcellular localization

The ORF of *TcMYB76* containing a termination codon was amplified from the pMD18-TcMYB73 plasmid using primers SL-TcMYB73-F/R (Additional file 4). The amplified fragment was inserted into the pHB-EGFP vector at the *Hind* III restriction sites. The recombinant vector, and the empty vector control (pHB-EGFP) were separately introduced into *A. tumefaciens* strain GV3101. Transformed bacterial cells were subsequently employed to infiltrate leaves of 4-week-old *N. benthamiana* plants via a standardized agroinfiltration protocol [46]. After 48–72 h of incubation, the infiltrated leaf epidermis were dissected and examined for GFP fluorescence using a Leica fluorescence microscope under 10 × 20 magnification (Leica Microsystems, Wetzlar, GmBH).

Generation of overexpression and RNAi constructs and transformation of *T. chinensis* needles

The full-length *TcMYB73* sequence was amplified from the pMD18-TcMYB73 plasmid using primers OE-TcMYB73-F/R (Additional file 4) and subcloned into the pHB-3xFLAG-EGFP vector at the *Bam*HI and *Sac*I restriction sites to generate the overexpression vector TcMYB73-OE. For RNAi, a 354 bp coding sequence (CDS) fragment of *TcMYB73* (+ 314 to + 667) was cloned in forward and reverse orientations into the pHANNIBAL vector to produce an intron-spliced hairpin RNA (RNAi construct). Then RNAi cassette was amplified using primers RNAi-TcMYB73-F/R (Additional file 4) and cloned into the pCAMBIA1300 vector at the *Eco*RI and *Bam*HI restriction sites, yielding the RNAi vector TcMYB73-RNAi.

The recombinant constructs were introduced into GV3101. Strains harboring TcMYB73-OE or the empty pHB-3xFLAG-EGFP (control), as well as TcMYB73-RNAi or the empty pCAMBIA1300 (additional control), were transformed into *T. chinensis* needles following the protocol of Chen et al. [27]. Briefly, the constructs, TcMYB73-OE, TcMYB73-RNAi, and empty vectors, were separately introduced into *Taxus* needles via GV3101. For transient transformations, single colonies of GV3101 harboring these vectors were cultured in 50 mL of YEB medium until reaching an OD600 of 0.6–0.8. Bacterial cells were subsequently centrifuged and resuspended in 50 mL of half-strength MS liquid medium supplemented with 200 μM acetosyringone. Fresh leaves were excised from the apical regions of two-year-old *T. chinensis* potted plants. Following surface sterilization, sterile scalpels were used to generate micro-incisions on the abaxial leaf surfaces to facilitate *Agrobacterium* infiltration. The wounded leaves were immersed in the bacterial suspension and agitated at 125 rpm for 12 h in darkness at 25 °C. Post-infection, needles were incubated on half-strength MS solid medium for 24 h at 25℃ in darkness. Harvested needles were divided into two subsets: one subset was submerged in liquid nitrogen and stored at −80℃ for subsequent analyses, while the other subset was transferred to moistened filter paper and maintained at 25℃ for 6 days to quantify taxane content. *T. chinensis* callus transformations were conducted according to the method outlined by Cao et al. [34]. All experiments were validated at least three biological replicates.

Cloning and promoter analysis of the 5′-Flanking Sequences of *TcT10OH*, *TcMYB73* and *TcWRKY33* Genes

The cloning of the 5′-flanking sequences of genes are conducted using the protocol described by Chen et al. [27]. Briefly, the CDS of *TcT10OH*, *TcMYB73* and *TcWRKY33* from *T. chinensis* were aligned with the entire genome sequence of *T. chinensis*. Subsequently, the 5′-untranslated regions (UTRs) and partial ORF sequences of these genes were obtained (Additional file 5). To ensure the accuracy of the 5′-flanking sequences, forward primers were designed based the predicted 5′-UTRs, while the reverse primers were designed according to the ORF sequences of those genes. Using genomic DNA from *T. chinensis* as the template, PCR products were amplified and then subjected to T/A cloning and sequencing. Only sequences encompassing the 5′-UTRs and partial ORF were deemed valid. Subsequently, the sequenced 5′-flanking regions were analyzed using the online tools PlantCare (http://bioinformatics.psb.ugent.be/webtools/plantcare/html/) and PLACE (http://www.dna.affrc.go.jp/PLACE/signalscan.html) to identify the core *cis*-elements and putative MREs within the promoters.

Quantitative real-time PCR

Quantitative real-time PCR was performed using ChamQ Universal SYBR qPCR Master Mix (Vazyme, Nanjing, China) and a CFX96 Touch Real-Time PCR Detection System (BIO-RAD, USA). The *TcGAPDH* sequence severed as an internal reference gene, and the relative fold differences in gene expression were calculated via the comparative cycle threshold method ($2^{-\Delta\Delta Ct}$) [47]. All experiments were executed in triplicate, and statistical significance was assessed using Student's *t*-test. The primer sequences are list in Additional file 4.

Liquid chromatography-mass spectrometry analysis of taxanes

For LC–MS analysis of taxanes, including 10-DAB III, baccatin III, and paclitaxel, treated *Taxus* needles were

collected, lyophilized, and homogenized into a fine powder in liquid nitrogen. Taxane extraction and quantification were conducted via LC–MS according to our previously described methods [34]. Three biological replicates were conducted to ensure analytical rigor.

Yeast one-hybrid assays

For prey vector construction, the *TcMYB73* gene was subcloned into the pJG4-5 vector via *Eco*RI and *Xho*I restriction sites, generating an AD:TcMY73 recombinant vector. For bait vectors, 250—450 bp fragments containing MREs were amplified from each promoter using gene-specific primers (Additional file 4) and ligated into pLacZ (2μ) vector using *Eco*RI and *Xho*I restriction sites, yielding constructs such as pLacZ-TcT10OHpro and pLacZ-TcWRKY33pro. Mutations in the MRE sites of the *TcT10OH* and *TcWRKY33* promoters within these constructs were introduced using the Hieff Mut™ Site-Directed Mutagenesis Kit (Yeasen). Finally, each bait vector was co-transformed with the prey vector into yeast strain EGY48. Transformants were plated onto SD/-Trp/-Ura/Gal/Raf agar medium supplemented with 80 mM X-gal and incubated for 3–5 days. Bait vectors co-transformed with the empty pJG4-5 vector served as negative controls.

Chromatin immunoprecipitation PCR

ChIP was carried out using transgenic *Taxus* needles expressing 35S:GFP-TcMYB73, following the method described in the literature [34]. ChIP DNA products were analyzed via qPCR with custom-designed primers targeting promoter regions of the *TcT10OH* and *TcWRKY33* genes. Primer pairs MRE1-F/MRE1-R, and MRE2-F/MRE2-R were employed amplify DNA fragments within the *TcT10OH* and *TcWRKY33* promoters, respectively (Additional file 4). All experiments were conducted in triplicate to validate reproducibility.

Electrophoretic mobility shift assays

The N-terminal coding sequence of *TcMYB73* (1–384 bp, encompassing the Myb-like DNA-binding domain) was amplified via PCR and ligated into the pGEX-4 T-1 vector (Amersham Biosciences) to generate a GST fusion construct in the correct reading frame. The engineered pGEX-TcMYB73 N vector was transformed into *Escherichia coli* Rosetta (DE3) cells to enable heterologous protein production. Once the culture reached an OD600 of 0.6–0.8, cells were induced with 0.2 mM isopropyl β-D-1-thiogalactopyranoside (IPTG) and incubated at 18 °C for 16 h to facilitate fusion protein synthesis. Recombinant protein purification was achieved using GST Sepharose 4 FF affinity chromatography (BBI). Protein size was verified by western blotting with an anti-GST antibody (BBI). EMSA assays were performed as previously described [48]. Biotinylated and unlabeled synthetic oligonucleotides (30 bp) corresponding to the *TcT10OH* and *TcWRKY33* promoter regions were synthesized. EMSA reactions utilized biotin-labeled probes and the LightShift Chemiluminescent EMSA Kit (Thermo Fisher Scientific), adhering to the manufacturer's guidelines. Briefly, assay mixtures were incubated for 20 min at 22 °C, followed by resolution on a 10% native polyacrylamide gel. Post-electrophoresis cross-linking enabled chemiluminescent detection of the biotin-labeled probes. Primer sequences for EMSA are detailed in Additional File 4.

Activity validation of the *TcMYB73* Gene

To assess the transcriptional activity of TcMYB73, Dual-LUC assays were conducted following a previously reported method with slight modifications [49]. The effector plasmid pBD-TcMYB73 was constructed by cloning the CDS of *TcMYB73* into the pBD vector. The empty pBD plasmid served as the negative control, while the pBD-VP16 plasmid, harboring the VP16 activation domain, functioned as the positive control. The reporter plasmid pGreenII-0800-LUC features five tandem copies of the GAL4-binding domain upstream of the minimal CaMV35S promoter and the LUC gene, coupled with an internal *Renilla* (REN) luciferase control under the regulation of the 35S promoter. Both reporter and effector plasmids were transformed into GV3101 (pSoup-p19). Tobacco leaves were transiently co-infiltrated with a combination of effector and reporter plasmids. Luciferase activity was quantified 72 h post-infiltration employing a dual-luciferase reporter assay kit (Promega). The transcriptional activation capacity of TcMYB73 was determined by assessing the relative LUC/REN ratio.

Transient dual-luciferase reporter assays

For the dual-luciferase activity assay, the native ~1500 bp promoter regions of *TcT10OH* and *TcWRKY33* were ligated into the pGreenII-0800-LUC vector using *HindIII* and *NcoI* restriction sites, generating the reporter constructs pGreenII-TcT10OHpro and pGreenII-TcWRKY33pro (Additional file 4). Mutations in the MRE sites of the *TcT10OH* and *TcWRKY33* promoters were engineered in these constructs using the Hieff Mut™ Site-Directed Mutagenesis Kit (Yeasen). Then, ORF of *TcMYB73* was amplified via PCR with *Hind*III and *Nco*I sites and subcloned into the pGreenII-62-SK vector to generate *TcMYB73*::pGreenII-62-SK effector vector (Additional file 4). Reporter and effector constructs were co-infiltrated into tobacco leaves using GV3101 (pSoup-p19). Infiltrated plants were incubated in darkness for 12 h in a greenhouse, followed

by cultivation under ambient conditions for 36–48 h. Luciferase activity was then quantified with a dual-luciferase reporter assay kit (Promoge). All assays were conducted in triplicate.

Abbreviations

SA	Salicylic acid
RNAi	RNA interference
TASY	Taxadiene synthase
DBAT	10-Deacetylbaccatin-III-10-O-acetyltransferase
DBTNBT	3′-*N*-Debenzoyl-2′-deoxytaxol-*N*-benzoyltransferase
Y1H	Yeast one-hybrid
EMSA	Electrophoretic Mobility Shift Assay
ChIP-qPCR	ChIP-quantitative polymerase chain reaction
Dual-LUC	Dual-luciferase
MRE	MYB recognition element
10-DAB	10-Deacetyl-baccatin III
GGPP	Geranylgeranyl pyrophosphate
TAT	Taxadienol 5α-O-acetyl transferase
PAM	Phenylalanine aminomutase
C_OA	Coenzyme A
BAPT	Baccatin III:3-animo-3-phenylpropanoyl transferase
JA	Jasmonic acid
MeJA	Methyl jasmonate
TF	Transcription factor
qPCR	Quantitative real-time PCR
Y2H	Yeast two-hybrid
BiFC	Bimolecular fluorescence complementation
SD	Standard deviation
MEP	Methylerythritol phosphate
CDS	Coding sequence
ORF	Open reading frame
MW	Molecular weight
pI	Isoelectric point
UTRs	Untranslated regions
LC–MS	Liquid chromatography-mass spectrometry
ChIP	Chromatin immunoprecipitation
LUC	Luciferase; DW: dry weight
TBT	Taxane 2α-O-benzoyl transferase
T5OH	Taxane 5α-hydroxylase
T7OH	Taxane 7β-hydroxylase
T2OH	Taxane 2α-hydroxylase
T10OH	Taxane 10β-hydroxylase
T13OH	Taxane 13α-hydroxylase
PCL	Phenylalanoyl CoA ligase
IPTG	Isopropyl β-D-1-thiogalactopyranoside

Supplementary Information

The online version contains supplementary material available at https://doi.org/10.1186/s12870-025-06755-9.

Additional file 1: Fig. S1 Phylogenetic tree of TcMYB73, and MYBs from Taxus chinensis and Arabidopsis.

Additional file 2: Fig. S2 Expression pattern of TcMYB73 (a), TcTASY (b), TcT10OH (c), TcDBAT (d), TcDBTNBT (e), and TcWRKY33 (b) genes in different tissues of T. chinensis.

Additional file 3: Fig. S3 Amino acid sequence alignment of TcMYB29a and several reported R2R3-MYBs in Taxus.

Additional file 4: Table S1 The primers used in this study.

Additional file 5: Promoter sequences.

Acknowledgements
Not applicable.

Authors' contributions
XC, and WW planned and designed the research. WW and XC wrote the manuscript. XW, WZ, DL, YR, and WW conducted the research and analyzed the data. All authors read and approved the final manuscript.

Funding
This work was supported by the National Natural Science Foundation of China (No. 82204344) and the Basic Research Program of Xuzhou (No. KC21028).

Data availability
No datasets were generated or analysed during the current study.

Declarations

Ethics approval and consent to participate
Not applicable.

Consent for publication
Not applicable.

Competing interests
The authors declare no competing interests.

Author details
[1]School of Life Science, Jiangsu Normal University, Xuzhou, Jiangsu 221116, People's Republic of China.

Received: 23 December 2024 Accepted: 20 May 2025
Published online: 28 May 2025

References

1. Sati P, Sharma E, Dhyani P, Attri DC, Rana R, Kiyekbayeva L, et al. Paclitaxel and its semi-synthetic derivatives: comprehensive insights into chemical structure, mechanisms of action, and anticancer properties. Eur J Med Res. 2024;29(1):90. https://doi.org/10.1186/s40001-024-01657-2.
2. Jamileh K, Ayuob A, Banafsheh S, Jaleh B, Seyed HR, Soodabeh D. Aptamer-conjugated gold nanoparticles for targeted paclitaxel delivery and photothermal therapy in breast cancer. J Drug Deliv Sci Technol. 2022;67:102954. https://doi.org/10.1016/j.jddst.2021.102954.
3. Wani MC, Horwitz SB. Nature as a remarkable chemist: a personal story of the discovery and development of Taxol. Anticancer Drugs. 2014;25(5):482–7. https://doi.org/10.1097/CAD.0000000000000063.
4. Howat S, Park B, Oh IS, Jin YW, Lee EK, Loake GJ. Paclitaxel: biosynthesis, production and future prospects. N Biotechnol. 2014;31(3):242–5. https://doi.org/10.1016/j.nbt.2014.02.010.
5. Baloglu E, Kingston DG. A new semisynthesis of paclitaxel from baccatin III. J Nat Prod. 1999;62(7):1068–71. https://doi.org/10.1021/np990040k.
6. Sung H, Ferlay J, Siegel RL, Laversanne M, Soerjomataram I, Jemal A, et al. Global cancer statistics 2020: GLOBOCAN estimates of incidence and mortality worldwide for 36 cancers in 185 countries. CA Cancer J Clin. 2021;71(3):209–49. https://doi.org/10.3322/caac.21660.
7. Sabzehzari M, Zeinali M, Naghavi MR. Alternative sources and metabolic engineering of taxol: Advances and future perspectives. Biotechnol Adv. 2020;43:107569. https://doi.org/10.1016/j.biotechadv.2020.107569.
8. da Hao C, Yang L, Huang B. Molecular evolution of paclitaxel biosynthetic genes *TS* and *DBAT* of *Taxus* species. Genetica. 2009;135(2):123–35. https://doi.org/10.1007/s10709-008-9257-7.
9. Long RM, Lagisetti C, Coates RM, Croteau RB. Specificity of the N-benzoyl transferase responsible for the last step of taxol biosynthesis. Arch Biochem Biophys. 2008;477(2):384–9. https://doi.org/10.1016/j.abb.2008.06.021.
10. Xiong X, Gou J, Liao Q, Li Y, Zhou Q, Bi G, et al. The *Taxus* genome provides insights into paclitaxel biosynthesis. Nat Plants. 2021;7(8):1026–36. https://doi.org/10.1038/s41477-021-00963-5.
11. Cheng J, Wang X, Liu X, Zhu X, Li Z, Chu H, et al. Chromosome-level genome of Himalayan yew provides insights into the origin and evolution of the paclitaxel biosynthetic pathway. Mol Plant. 2021;14(7):1199–209. https://doi.org/10.1016/j.molp.2021.04.015.

12. Fu F, Song C, Wen C, Yang L, Guo Y, Yang X, et al. The *Metasequoia* genome and evolutionary relationships among redwoods. Plant Commun. 2023;4(6):100643. https://doi.org/10.1016/j.xplc.2023.100643.
13. Jiang B, Gao L, Wang H, Sun Y, Zhang X, Ke H, et al. Characterization and heterologous reconstitution of *Taxus* biosynthetic enzymes leading to baccatin III. Science. 2024;383(6683):622–9. https://doi.org/10.1126/science.adj3484.
14. Tong Y, Luo Y, Gao W. Biosynthesis of paclitaxel using synthetic biology. Phytochem Rev. 2022;21:863–77. https://doi.org/10.1007/s11101-021-09766-0.
15. Hou S, Tsuda K. Salicylic acid and jasmonic acid crosstalk in plant immunity. Essays Biochem. 2022;66(5):647–56. https://doi.org/10.1042/EBC20210090.
16. Wang JW, Wu JY. Nitric oxide is involved in methyl jasmonate-induced defense responses and secondary metabolism activities of *Taxus* cells. Plant Cell Physiol. 2005;46(6):923–30. https://doi.org/10.1093/pcp/pci098.
17. Lenka SK, Boutaoui N, Paulose B, Vongpaseuth K, Normanly J, Roberts SC, et al. Identification and expression analysis of methyl jasmonate responsive ESTs in paclitaxel producing *Taxus cuspidata* suspension culture cells. BMC Genomics. 2012;13:148. https://doi.org/10.1186/1471-2164-13-148.
18. Li S, Zhang P, Zhang M, Fu C, Zhao C, Dong Y, et al. Transcriptional profile of *Taxus chinensis* cells in response to methyl jasmonate. BMC Genomics. 2012;13:295. https://doi.org/10.1186/1471-2164-13-295.
19. Jiang L, Zhang K, Lü X, Yang L, Wang S, Chen D, et al. Characterization and expression analysis of genes encoding taxol biosynthetic enzymes in *Taxus* spp. J For Res. 2021;32:2507–15. https://doi.org/10.1007/s11676-021-01290-3.
20. Li S, Zhang P, Zhang M, Fu C, Yu L. Functional analysis of a WRKY transcription factor involved in transcriptional activation of the DBAT gene in *Taxus chinensis*. Plant Biol (Stuttg). 2013;15(1):19–26. https://doi.org/10.1111/j.1438-8677.2012.00611.x.
21. Chen L, Wu L, Yang L, Yu H, Huang P, Wang Y, et al. TcJAV3-TcWRKY26 cascade is a missing link in the jasmonate-activated expression of taxol biosynthesis gene *DBAT* in *Taxus chinensis*. Int J Mol Sci. 2022;23(21):13194. https://doi.org/10.3390/ijms232113194.
22. Lenka SK, Nims NE, Vongpaseuth K, Boshar RA, Roberts SC, Walker EL. Jasmonate-responsive expression of paclitaxel biosynthesis genes in *Taxus cuspidata* cultured cells is negatively regulated by the bHLH transcription factors TcJAMYC1, TcJAMYC2, and TcJAMYC4. Front Plant Sci. 2015;6:115. https://doi.org/10.3389/fpls.2015.00115.
23. Zhang M, Li S, Nie L, Chen Q, Xu X, Yu L, et al. Two jasmonate-responsive factors, TcERF12 and TcERF15, respectively act as repressor and activator of *tasy* gene of taxol biosynthesis in *Taxus chinensis*. Plant Mol Biol. 2015;89(4–5):463–73. https://doi.org/10.1007/s11103-015-0382-2.
24. Zhao Z, Zhang Y, Li W, Tang Y, Wang S. Transcriptomics and physiological analyses reveal changes in paclitaxel production and physiological properties in *Taxus cuspidata* suspension cells in response to elicitors. Plants (Basel). 2023;12(22):3817. https://doi.org/10.3390/plants12223817.
25. Yu L, Lan W, Qin W, Xu H. Effects of salicylic acid on fungal elicitor-induced membrane-lipid peroxidation and taxol production in cell suspension cultures of *Taxus chinensis*. Process Biochem. 2001;5(37):477–82. https://doi.org/10.1016/S0032-9592(01)00243-6.
26. Sarmadi M, Karimi N, Palazón J, Ghassempour A, Mirjalili MH. The effects of salicylic acid and glucose on biochemical traits and taxane production in a *Taxus baccata* callus culture. Plant Physiol Biochem. 2018;132:271–80. https://doi.org/10.1016/j.plaphy.2018.09.013.
27. Chen Y, Zhang H, Zhang M, Zhang W, Ou Z, Peng Z, et al. Salicylic acid-responsive factor TcWRKY33 positively regulates taxol biosynthesis in *Taxus chinensis* in direct and indirect ways. Front Plant Sci. 2021;12:697476. https://doi.org/10.3389/fpls.2021.697476.
28. Zhang M, Dong Y, Nie L, Lu M, Fu C, Yu L. High-throughput sequencing reveals miRNA effects on the primary and secondary production properties in long-term subcultured *Taxus* cells. Front Plant Sci. 2015;6:604. https://doi.org/10.3389/fpls.2015.00604.
29. Ying C, Meng Z, Wenli Z, Yamin W, Hua Z, Liu Y, et al. MiR5298b regulated taxol biosynthesis by acting on TcNPR3, resulting in an alleviation of the strong inhibition of the TcNPR3-TcTGA6 complex in *Taxus chinensis*. Int J Biol Macromol. 2023;248:125909. https://doi.org/10.1016/j.ijbiomac.2023.125909.
30. Dubos C, Stracke R, Grotewold E, Weisshaar B, Martin C, Lepiniec L. MYB transcription factors in *Arabidopsis*. Trends Plant Sci. 2010;15(10):573–81. https://doi.org/10.1016/j.tplants.2010.06.005.
31. Tong Y, Xue J, Li Q, Zhang L. A generalist regulator: MYB transcription factors regulate the biosynthesis of active compounds in medicinal plants. J Exp Bot. 2024;75(16):4729–44. https://doi.org/10.1093/jxb/erae225.
32. Arce-Rodríguez ML, Ochoa-Alejo N. An R2R3-MYB transcription factor regulates capsaicinoid biosynthesis. Plant Physiol. 2017;174(3):1359–70. https://doi.org/10.1104/pp.17.00506. (Epub 2017 May 8).
33. Yu C, Luo X, Zhang C, Xu X, Huang J, Chen Y, et al. Tissue-specific study across the stem of *Taxus media* identifies a phloem-specific TmMYB3 involved in the transcriptional regulation of paclitaxel biosynthesis. Plant J. 2020;103(1):95–110. https://doi.org/10.1111/tpj.14710.
34. Cao X, Xu L, Li L, Wan W, Jiang J. TcMYB29a, an ABA-Responsive R2R3-MYB transcriptional factor, upregulates taxol biosynthesis in *Taxus chinensis*. Front Plant Sci. 2022;13:804593. https://doi.org/10.3389/fpls.2022.804593.
35. Yu C, Huang J, Wu Q, Zhang C, Li XL, Xu X, et al. Role of female-predominant MYB39-bHLH13 complex in sexually dimorphic accumulation of taxol in *Taxus media*. Hortic Res. 2022;9:uhac062. https://doi.org/10.1093/hr/uhac062.
36. Zhan X, Zhang H, Liang X, Hou K, Lin W, Ma R, et al. Single-cell ATAC sequencing illuminates the cis-regulatory differentiation of taxol biosynthesis between leaf mesophyll and leaf epidermal cells in *Taxus mairei*. Ind Crops Prod. 2023. https://doi.org/10.1016/j.indcrop.2023.117411.
37. Yu C, Hou K, Zhang H, Liang X, Chen C, Wang Z, et al. Integrated mass spectrometry imaging and single-cell transcriptome atlas strategies provide novel insights into taxoid biosynthesis and transport in *Taxus mairei* stems. Plant J. 2023;115(5):1243–60. https://doi.org/10.1111/tpj.16315.
38. Hu X, Zhang L, Wilson I, Shao F, Qiu D. The R2R3-MYB transcription factor family in *Taxus chinensis*: identification, characterization, expression profiling and posttranscriptional regulation analysis. PeerJ. 2020;8:e8473. https://doi.org/10.7717/peerj.8473.
39. Onrubia M, Moyano E, Bonfill M, Palazón J, Goossens A, Cusidó RM. The relationship between *TXS*, *DBAT*, *BAPT* and *DBTNBT* gene expression and taxane production during the development of *Taxus baccata* plantlets. Plant Sci. 2011;181(3):282–7. https://doi.org/10.1016/j.plantsci.2011.06.006.
40. Wheeler NC, Jech K, Masters S, Brobst SW, Alvarado AB, Hoover AJ, et al. Effects of genetic, epigenetic and environmental factors on taxol content in *Taxus brevifolia* and related species. J Nat Prod. 1992;55(4):432–40. https://doi.org/10.1021/np50082a005.
41. Cameron SI, Smith RF. Seasonal changes in the concentration of major taxanes in the biomass of wild canada yew (*Taxus canadensis* Marsh). Pharm Biol. 2008;46(1–2):35–40. https://doi.org/10.1080/13880200701729760.
42. Nasiri J, Naghavi MR, Alizadeh H, Moghadam MR. Seasonalbased temporal changes fluctuate expression patterns of *TXS*, *DBAT*, *BAPT* and *DBTNBT* genes alongside production of associated taxanes in *Taxus baccata*. Plant Cell Rep. 2016;35(5):1103–19. https://doi.org/10.1007/s00299-016-1941-y.
43. Liu Z, Yu LJ, Li MT, Zhu M, Zhu L. Sites of taxol and its precursor biosynthesis and accumulation in *Taxus chinensis*. J Huazhong Agric Univ. 2006;25(3):313–7 ((in Chinese)).
44. Kaspera R, Croteau R. Cytochrome P450 oxygenases of taxol biosynthesis. Phytochem Rev. 2006;5(2–3):433–44. https://doi.org/10.1007/s11101-006-9006-4.
45. Lee EK, Jin YW, Park JH, Yoo YM, Hong SM, Amir R, et al. Cultured cambial meristematic cells as a source of plant natural products. Nat Biotechnol. 2010;28(11):1213–7. https://doi.org/10.1038/nbt.1693.
46. Gui J, Zheng S, Shen J, Li L. Grain setting defect1 (GSD1) function in rice depends on S-acylation and interacts with actin 1 (OsACT1) at its C-terminal. Front Plant Sci. 2015;6:804. https://doi.org/10.3389/fpls.2015.00804.
47. Livak K, Schmittgen T. Analysis of relative gene expression data using real-time quantitative PCR and the $2^{-\Delta\Delta Ct}$ Method. Methods. 2001;25(4):402–8. https://doi.org/10.1006/meth.2001.1262.
48. Wang CC, Meng LH, Gao Y, Grierson D, Fu DQ. Manipulation of light signal transduction factors as a means of modifying steroidal glycoalkaloids accumulation in tomato leaves. Front Plant Sci. 2018;12(9):437. https://doi.org/10.3389/fpls.2018.00437.
49. Lu S, Zhang Y, Zhu K, Yang W, Ye J, Chai L, et al. The citrus transcription factor CsMADS6 modulates carotenoid metabolism by directly regulating carotenogenic genes. Plant Physiol. 2018;176(4):2657–76. https://doi.org/10.1104/pp.17.01830.

Publisher's Note